Author(s): Moilanen, Jani; Power, Philip; Tuononen, Heikki

Title: Nature of Bonding in Group 13 Dimetallenes: a Delicate Balance between Singlet Diradical Character and Closed Shell Interactions

Year: 2010

Version:

Please cite the original version:

Moilanen, J., Power, P., & Tuononen, H. (2010). Nature of Bonding in Group 13 Dimetallenes: a Delicate Balance between Singlet Diradical Character and Closed Shell Interactions. Inorganic Chemistry, 49(23), 10992-11000. https://doi.org/10.1021/ic101487g

Nature of Bonding in Group 13 Dimetallenes: a Delicate Balance between Singlet Diradical Character and Closed Shell Interactions

Jani Moilanen,[a] Philip P. Power[b] and Heikki M. Tuononen[a,*]

[a] *Department of Chemistry, P.O. Box 35, FI-40014 University of Jyväskylä, Finland.*

[b] *Department of Chemistry, University of California, One Shield Avenue, Davis, CA, 95616, USA.*

* Corresponding author:

Phone: +358-14-260-2618; Fax: +358-14-260-2501; E-mail: heikki.m.tuononen@jyu.fi

Abstract

The nature of metal–metal bonding in group 13 dimetallenes REER (E = Al, Ga, In, Tl; R = H, Me, ^{t}Bu, Ph) was investigated by use of quantum chemical methods that include HF, second order Møller-Plesset perturbation theory (MP2), coupled cluster **(**CCSD(T)), complete active space with (CASPT2) and without (CAS) second order perturbation theory and two density functionals, namely B3LYP and M06-2X. The results show that the metal–metal interaction in group 13 dimetallenes stems almost exclusively from static and dynamic electron correlation effects: both dialuminenes and digallenes have an important singlet diradical component in their wave function, whereas the bonding in the heavier diindenes and, in particular, dithallenes is dominated by closed shell metallophilic interactions. The reported calculations represent the first systematic attempt to determine the metal and ligand dependent bonding changes in these systems.

1 Introduction

The current widespread interest in multiple bonding between heavier main group elements stems from several landmark papers in the 1970s and 1980s which disclosed the first stable species containing multiple bonds between heavier group 14[1,2] and 15 elements.[3] The principles underlying the bonding in these systems were explained in an important 1984 review of the area.[4] Since then, a plethora of multiple bonded heavier main group derivatives of group 14 and 15 elements have been synthesized, and their bonding analyzed in detail.[5]

For many years, it was thought that the electron deficient nature of group 13 elements precluded the formation of homonuclear multiple bonds. However, in the 1980s, a number of groups showed that multiple bonds between boron atoms could be generated by reduction of tetraorganodiboron species.[6] By using a similar approach, it was shown in 1993 that the reduction of the heavier R_2EER_2 (E= Al or Ga) congeners gave monoanion radicals $[R_2EER_2]^{\bullet-}$ with a formal π-bond order of one half.[7] X-ray crystallography confirmed the shortening of the bond upon reduction as well as small torsion angles between the metal coordination planes, consistent with the formation of an E–E π-interaction. Attempted reduction to give the dianions $[R_2E{=}ER_2]^{2-}$ led to rearrangements to form the $[E(ER_2)_3]^{2-}$ species.[8] The related neutral radical $[R_2GaGaR]^{\bullet}$ and the anion $[R_2GaGaR]^-$ (R = $Si(^tBu)_3$) were also characterized,[9] and they displayed a significant shortening of the Ga–Ga bond in comparison to R_2GaGaR_2. The synthesis of $Na_2[RGaGaR]$ (R = C_6H_3-2,6-(C_6H_2-2,4,6-$^iPr_3$)$_2$ in 1997 demonstrated that also the heavier group 13 element alkyne analogues could be stabilized.[10] However, the electronic structure of the digallyne proved controversial: the –CGaGaC– array had a markedly trans-bent structure with bridging Na^+ ions and a rather long Ga–Ga bond length of 2.319 Å. This initiated a lively debate regarding the Ga–Ga bond order, but various theoretical approaches yielded different answers to the question.[11] An attempt to resolve the problem led to the synthesis of a neutral digallene, RGaGaR, which was predicted to contain a Ga–Ga double bond based on the assumption of a Ga≡Ga triple bond in $Na_2RGaGaR$.

The crystal structure of the first digallene (R = C_6H_3-2,6-(C_6H_3-2,6-$^iPr_2$)$_2$) was reported in 2002 and it had a trans-bent structure with a Ga–Ga distance of 2.627 Å *i.e.* much longer than a typical single bond.[12] Moreover, cryoscopy suggested that, like the tetrahedral gallium clusters, $(GaR)_4$,[13] the molecule dissociated to GaR monomers in solution. Thus, both structural and physical data indicated

that the Ga–Ga bond order is much less than one, which is inconsistent with the existence of a Ga–Ga triple bond in the digallyne. The weakness of the Ga–Ga bond is underlined by the isolation of GaR monomers with use of slightly bulkier ligands.[14] The heavier In[15] and Tl[16] dimetallenes are known to adopt similar trans-bent structures with elongated E–E bonds in the solid state and they also dissociate to monomers in solution. All attempts to characterize a dialuminene, RAlAlR, have led to a cycloaddition reaction between the putative dimetallene and the solvent.[17]

The trans-bent structures of group 13 dimetallenes have been rationalized using the orbital-based donor-acceptor model.[18] Recent density functional theory (DFT) calculations for the experimentally characterized digallenes revealed that the Ga–Ga bond is a good deal weaker than a conventional single bond and similar in strength to closed shell, metallophilic, interactions.[14] Yet, it is not immediately apparent how DFT in its standard formalism completely describes the bonding in these molecules since it does not account for dispersion effects which play a key role in closed shell interactions.[19] A simple explanation is to assume that there is a small, albeit important, covalent (orbital) component to the bonding which is captured and accurately reproduced by the theory. The bonding debate on dimetallenes and dimetallynes has in many instances focused on the role of the so-called "slipped π-type orbital",[11a-d] which is the highest occupied molecular orbital (HOMO) in dimetallenes. It is not widely realized that this orbital is formally antibonding with respect to the metal–metal bond,[11d] although there is a small secondary bonding interaction in between the lone pair on the group 13 element and the E–R bond facing it. Presumably the bonding and anti-bonding effects do not cancel out completely and afford a small net bonding component. However, if the resultant interaction is dominant, its effects should be visible also at the Hartree-Fock (HF) level. Contrary to these expectations, the HF method affords Ga–Ga bonds that are significantly elongated compared to those obtained experimentally or even leads to complete dissociation of the dimers.[11a,11d,18a]

It is clear that neither orbital interactions (the donor-acceptor model) nor closed shell attraction, or even a combination thereof, can offer a complete explanation of the bonding trends observed for group 13 dimetallenes. Consequently, we decided to conduct a thorough investigation of the nature of bonding in group 13 dimetallenes REER, **1**–**4** (E = Al, Ga, In, Tl; R = H, Me, ^{t}Bu, Ph) by using a variety of high-level quantum chemical methods. In the current contribution, the results of these investigations are described and it is shown how the bonding in group 13 dimetallenes involves a

delicate interplay between static and dynamic electron correlation effects.[20] The information from the electronic structure calculations is used in reinterpretation of the results from qualitative bonding analyses and the picture thus obtained provides a self-consistent and realistic representation of the bonding in group 13 dimetallenes.

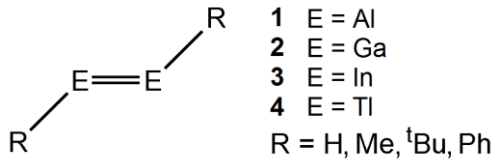

2 Computational Details

The geometries of **1**–**4** were optimized in C_{2h} symmetry using a variety of theoretical approaches: HF, second order perturbation theory (MP2),[21] coupled cluster (CCSD(T))[22] as well as complete active space without (CAS)[23] and with second order perturbation theory correction (CASPT2)[24]. In addition to ab initio methods, two density functionals, namely B3LYP[25] and M06-2X,[26] were also employed in the optimizations. Although the M06-2X functional is designed to take into account typical long-range non-covalent interactions which are expected to be of great importance for the heavier dimetallenes, it predicted several of the studied systems to be transition states on the potential energy hypersurface. Hence, the M06-2X results will not be discussed further in this paper. The performance of the B3LYP functional in combination with Grimme's empirical dispersion correction (DFT-D)[27] was also assessed. However, this approach could not be used for dithallenes, for which the dispersion effects are expected to be the most significant, as the required atomic parameters for thallium are currently nonexistent.

Due to the computational cost of the CASPT and CCSD(T) methods, geometry optimizations at these levels were done only for the hydrogen and methyl substituted derivatives. Frequency analyses were performed for optimized geometries to ensure that they correspond to true minima on the potential energy hypersurface. In multiconfigurational CAS and CASPT2 calculations, the active space (4,5) was chosen based on the results of full valence space (8,10) optimizations of parent dimetallenes. The HF MOs forming the active space are shown in Figure 1 for the parent dialuminene.

In all calculations, the correlation consistent polarized valence triple-ζ cc-pVTZ basis sets were used for the elements of the first four rows.[28] For the heavier elements indium and thallium, the valence

triple-ζ quality quasi-relativistic small core pseudopotential basis sets, namely cc-pVTZ-PP, were employed.[29] Although this approach is a simple and straightforward way to include scalar relativistic treatment of atoms in molecular calculations, it nevertheless omits all effects arising from spin-orbit coupling which are important for thallium. In correlated calculations, the outermost d-orbitals were excluded from the frozen core *i.e.* the largest noble gas core was used. However, for thallium, the electrons in the filled 4f-shell were not correlated as they are accounted for in the corresponding pseudopotential. In MP2 and CCSD(T) calculations, the well-established counterpoise procedure[30] was used to correct the results for basis set superposition error (BSSE). However, no BSSE correction was applied in case of multiconfigurational methods due to theoretical ambiguities in assigning an active space for the monomeric units. In addition, BSSE is expected to be minimal at the HF and DFT levels of theory as long as polarized triple-ζ quality basis sets are used.

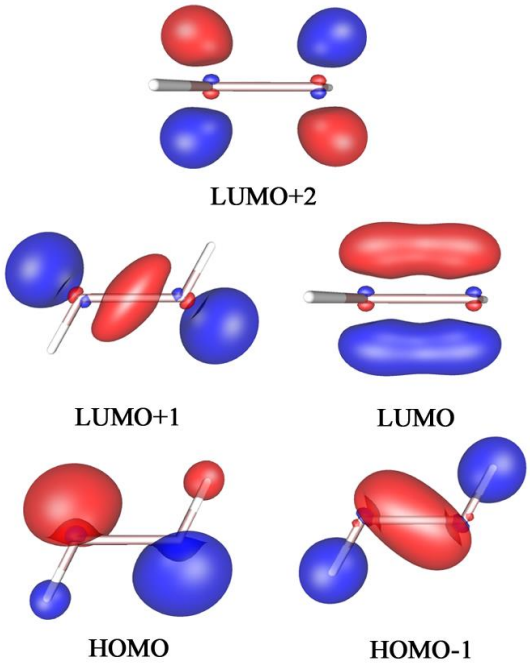

Figure 1. Frontier MOs of trans-bent dialuminenes (R = H) that were used as the active space in CAS and CASPT2 calculations.

The bonding in systems **1**–**4** was analyzed using two methods based on the total electron density: the theory of atoms in molecules (AIM)[31] and the analysis of the electron localization function (ELF).[32] These analyses were performed using the electron density obtained from the B3LYP/cc-pVTZ calculations.

All optimizations and frequency calculations were done with the Gaussian 09[33] and Molpro 2006.1[34] programs. The TopMod[35] program suite was used for performing electron density analyses, whereas the visualizations of molecular orbitals and ELFs were done with gOpenMol.[36]

3 Results and Discussion

Optimized geometries and wave functions. The geometries of **1**–**4** (R = H, Me, ^{t}Bu, Ph) were calculated with different theoretical methods and the optimized structural parameters are given in Table 1 along with the literature values of some representative compounds. It is evident from the outset that from the three standard methods applied, namely HF, MP2 and DFT, the HF values deviate the most from the rest in Table 1. Clearly the orbital interaction alone does not provide a thorough explanation of bonding as the calculated HF bond lengths are off by at least 0.2 Å for all but the parent systems. Thus, the HF wave function underbinds the dimers, and it does it even to the extent that it predicts all dithallenes to be monomeric. Although not shown in Table 1, the HF method also predicts the experimentally observed digallenes and diindenes with m-terphenyl substituents to be unbound, which underlines the negligible contribution from zeroth order orbital interactions to bonding. In contrast to the HF results, the MP2 method and the B3LYP density functional predict molecular structures which are in good mutual agreement as well as reasonably close to the experimental data where available. It therefore seems straightforward to assume that the error in the HF results is primarily due to its inability to model closed shell interactions which arise mostly from dispersion *i.e.* from non-local dynamic electron correlation effects.[19] Such deficiency is readily compensated by the MP2 approach but not by the standard B3LYP functional,[19] which would make the good performance of DFT somewhat fortuitous. In order to investigate this phenomenon more deeply, detailed wave function analyses starting at the HF level of theory were performed for all systems **1**–**4**.

Table 1. Optimized Metal−Metal Bond Lengths (in Ångströms) for **1**–**4** at Different Levels of Theory

		HF	UHF	MP2	CCSD(T)	CAS	CASPT2	B3LYP[e]	exptl.
Al	H	2.78	2.57	2.65	2.65	2.68	2.62	2.67 (2.67)	
	Me	2.91	2.73	2.72	2.71	2.75	2.66	2.74 (2.75)	
	^{t}Bu	2.95	2.64	2.71	-	2.78	-	2.76 (2.75)	
	Ph	2.91	2.70	2.69	-	2.73	-	2.73 (2.73)	
Ga	H	2.79	2.65	2.55	2.57	2.66	2.50	2.64 (2.64)	
	Me	2.92	2.70	2.61	2.62	2.72	2.53	2.70 (2.71)	2.51[a] – 2.63[b]
	^{t}Bu	2.96	2.74	2.60	-	2.75	-	2.71 (2.70)	
	Ph	2.95	2.95	2.59	-	2.70	-	2.69 (2.68)	
In	H	3.34	3.33	2.97	2.99	3.10	2.88	3.06 (3.27)	
	Me	3.45	3.12	3.02	3.04	3.16	2.92	3.11 (3.31)	2.98[c]
	^{t}Bu	3.50	3.13	3.00	-	3.20	-	3.13 (3.30)	
	Ph	3.73	3.70	3.01	-	3.18	-	3.14 (3.32)	
Tl	H	*	*	3.17	3.25	3.69	3.01	3.26	
	Me	*	*	3.19	3.27	3.70	3.03	3.29	3.09[d]
	^{t}Bu	*	*	3.11	-	3.71	-	3.28	
	Ph	*	*	3.20	-	*	-	*	

* The optimized structure is not a minimum on the potential energy surface. [a] Reference 14. [b] Reference 12. [c] Reference 15. [d] Reference 16. [e] DFT-D values in parenthesis.

Calculations testing the stability of the HF solutions show that all but the dithallenes have restricted-unrestricted instabilities[37] and lower energy wave functions can be found by allowing the spatial parts of the α and β orbitals to differ. This indicates that the lighter group 13 dimetallenes have

singlet diradical character in their wave function and that multiconfigurational or coupled cluster methods should be used in order to obtain a balanced description of their electronic structures.[38,39] The presence of diradical character in **1**–**4** is consistent with the fact that similar static electron correlation effects have been well described and characterized for the heavier group 14 alkyne analogues.[40] However, the diradical component seems to be small in group 13 dimetallenes as judged by the closeness of the total energies from the two sets of calculations: the restricted and unrestricted HF solutions for **1**–**3** differ generally between 5 and 20 kJ mol^{-1}. This view is supported by the fact that broken symmetry solutions could not be located at the unrestricted B3LYP level as all calculations converged to spin-paired solutions. In the DFT formalism of electronic structure theory, static electron correlation effects such as singlet diradical character are primarily modeled by the exchange-correlation functional and not by the calculated reference determinant, which explains why restricted DFT is able to treat small to moderate amounts of diradical character and therefore provide an accurate description of systems which are known to be pathological cases for many of the traditional wave function based methods.[41]

The above results provide the first clue as to how DFT is able to model the structures of group 13 dimetallenes and digallenes in particular. Although the diradical character in **1**–**3** is small, it is significant compared to the total interaction strength. Hence, even though DFT in its standard formalism fails to capture closed shell interactions, it does a fine job in reproducing other components that are more important for bonding. Nevertheless, the lack of proper treatment of dispersion effects is one probable explanation for why B3LYP predicts too long metal–metal distances for dithallenes. An additional contributing factor is the exclusion of spin-orbit effects, which is supported by the fact that the high-level CCSD(T) method gives very similar geometries as B3LYP. In an attempt to include the effects of dispersion in the DFT calculations, the geometries of group 13 dimetallenes were re-optimized using an empirical correction procedure (DFT-D). As expected, the data for dialuminenes and digallenes are not affected by the correction (see Table 1), but the In–In bond length in diindenes is elongated by 0.2 Å upon inclusion of dispersion effects! This is a totally unexpected result as dispersion is a purely attractive force and its proper treatment should lead to contraction of the calculated bond lengths. Unfortunately, it was impossible to test the effect of the empirical dispersion correction on dithallenes due to methodological limitations (see above).

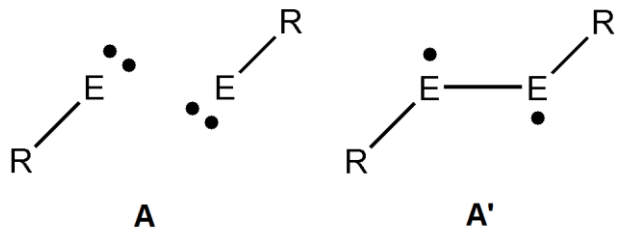

Quantum mechanically, the diradical character in group 13 dimetallenes means that their wave functions are not adequately described by a single HF determinant and, according to the stability analyses, they need at least one more determinant which transfers electrons from the E–E antibonding HOMO to the E–E bonding LUMO+1 (see Figure 1). This can be presented pictorially by drawing two Lewis structures **A** and **A'** which correspond to the RHF determinant and the singlet diradical component of the wave function, respectively. In light of the above data, the good performance of the MP2 method in predicting the geometries of lighter dimetallenes now seems striking as perturbation theory is known to be notoriously poor in describing static electron correlation effects that originate from near degeneracy of electronic configurations.[20] To this end, it was necessary to conduct more detailed wave function analyses using multiconfigurational (CAS and CASPT2) and coupled cluster (CCSD(T)) methods.

As the data in Table 1 show, the performance of the CAS method in predicting the geometries of **1**–**4** is significantly better than that observed for HF. The calculated metal–metal bond lengths are much closer to the experimental values though discrepancies yet remain. Most notably, some of the optimized bond lengths are still rather long, especially for the heavier congeners. This confirms that the closed shell interactions become increasingly important upon descending group 13 to the extent that they dominate the bonding in case of thallium. For indium, the relative importance of the two bonding contributions seems to be nearly equal as determined from the errors in the calculated metal–metal distances. However, for the lighter derivatives, a significant part of the total interaction can be recovered by using a CAS wave function that is a combination of only very few configurations. As expected,[20] the inclusion of dynamic electron correlation via the CASPT2 method leads to further shortening of the metal–metal distances which are now very close to the experimental values throughout the whole series. This is particularly true in case of the heaviest dimetallenes for which the

thallium–thallium bond length contracts as much as 0.7 Å when closed shell interactions are appropriately taken into account in calculations.

The weights of the excited determinants in the CAS wave function, *i.e.* the squares of the CI vector coefficients, give an estimate of the singlet diradical character in **1**–**4**.[42] In a perfect singlet diradical, both the HF and the doubly excited diradical determinant would have equal weights in the wave function. In such a case, the CI vector coefficients for the two configurations, C_{HF} and C_{DRCL}, are both $1/\sqrt{2}$. The diradical character can then be conveniently described with a simple relation $[C_{DRCL}^2/(1/\sqrt{2})^2] \times 100\% = 2C_{DRCL}^2 \times 100\%$. Using the above equation with the CI vector coefficients taken from the CAS wave functions, shown graphically in Figure 2, gives diradical character in between 14% and 6% for dimetallenes **1**–**3**, whereas it is insignificant, only 1%, for the dithallenes. The data in Figure 2 illustrate nicely that the C_{DRCL} coefficient and, hence, the diradical character varies only little with respect to the identity of the substituent and decreases stepwise when going down the group 13. These results are fully consistent with the conclusions drawn based on the optimized geometrical parameters alone.

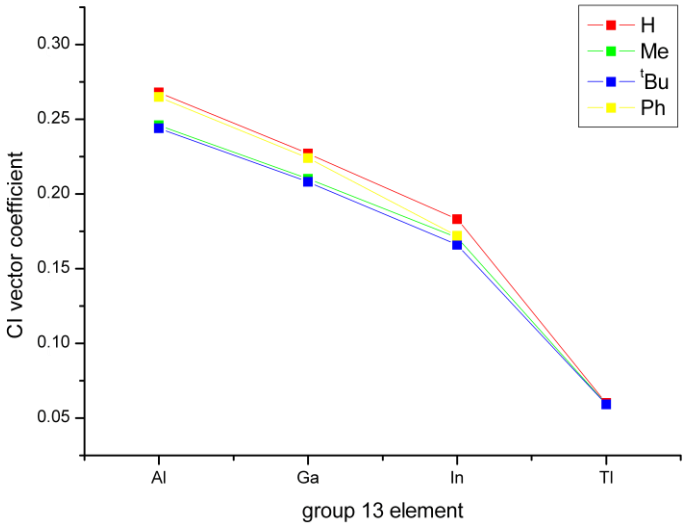

Figure 2. Calculated (CAS/cc-pVTZ) CI vector coefficients for **1**–**4**.

By virtue of the infinite-order feature of the coupled cluster (and the analogous quadratic configuration interaction (QCI)) method, it has the ability to handle static electron correlation in cases where the wave function still remains largely dominated by the HF determinant.[43] Since the singlet diradical character in **1**–**4** ranges from moderate (dialuminenes) to of no significant importance (dithallenes), it is not unexpected that the CCSD(T) method yields reasonably accurate geometric parameters for all group 13 dimetallenes (see Table 1). However, the almost equally good performance of the MP2 approach is yet without a convincing explanation. In order to compare the performance of the two computational approaches, it is illustrative to transform the calculated wave functions to the natural orbital basis and analyze the occupancies of the orbitals thus obtained. By definition, the natural orbitals are the eigenfunctions of the one-particle electron density matrix, whereas their occupancies are the eigenvalues of this matrix.[44] It can be shown that as the level of theory is increased, the natural orbital occupation numbers (NOONs) converge towards values that they adopt in the exact wave function, which allows their use as a benchmark of the quality of the approximation employed.[45]

The NOONs of dimetallenes **1**–**4** were calculated at the MP2 and QCISD(T) levels of theory. The QCISD(T) approach is essentially equivalent to the more familiar CCSD(T) method and was used only because the required orbital transformation has not been implemented to any of the employed program packages at the corresponding coupled cluster level.[46] The calculated NOONs reveal major differences between the wave functions given by the two methods. For example, at the MP2 level, a small amount of electron density in dimetallenes becomes equally distributed among the formally unoccupied orbitals that all have relatively small NOONs, between 0.02 and 0.05 electrons. Conversely, at the QCISD(T) level, the NOONs of **1** show a very uneven distribution. Most notably, the HOMO has a deficiency of roughly 0.20 electrons that have been transferred almost exclusively to the LUMO+1 with a NOON of 0.15 electrons. A similar trend is observed for the other dimetallenes **2**–**4** as well, but the amount of electrons transferred diminishes progressively upon descending group 13 and levels out in case of the dithallenes. Based on these data, it is straightforward to conclude that the QCISD(T) wave function, as well as its coupled cluster analog, mirror well the electronic structures of group 13 dimetallenes: the singlet diradical nature of the molecules is apparent from the calculated NOONs and the populations of the orbitals are in good agreement with the calculated diradical character based on the natural orbitals at the CAS level (see below). On the other hand, the MP2 method predicts electronic structures which are both qualitatively and quantitatively far off from the expected results. In fact, the MP2 natural

orbitals show an electronic distribution which is very typical for systems dominated by dynamic electron correlation effects alone. Taking this into account, the most likely explanation for the good performance of MP2 in predicting the structures of **1**–**4** is that the method simply overestimates the effects of dispersion and dynamic electron correlation in general, which it is known to do,[19,20] and therefore fortuitously gets the correct results for the wrong reasons.

The NOONs can also be used as another benchmark of diradical character.[47] In a perfect diradical, there would be two natural orbitals, each occupied by exactly one electron. Hence, a suitable index for diradical character can be obtained by comparing the occupation in the acceptor orbital n_{ACC} (formally the LUMO+1 in case of **1**–**4**) to the reference value of one electron *i.e.* (n_{ACC}/1.00) × 100%. For this purpose, the CAS wave functions were converted to the natural orbital basis and the orbital occupation numbers thus obtained are shown graphically in Figure 3. Translated to diradical character, the data in Figure 3 accurately reproduces the trend in CI vector coefficients (Figure 2): when calculated from the NOONs, the diradical character in **1**–**3** ranges between 15% and 6% while it is only 1% for **4**. In general, single configuration based methods such as RHF and MP2 are deemed insufficient to describe the system of interest whenever its multiconfigurational wave function contains NOONs greater than 0.1.[48] In case of group 13 dimetallenes, the aluminum and gallium systems are either very close to this threshold or even above it, which fully supports the conclusions on the singlet diradical character in these systems.

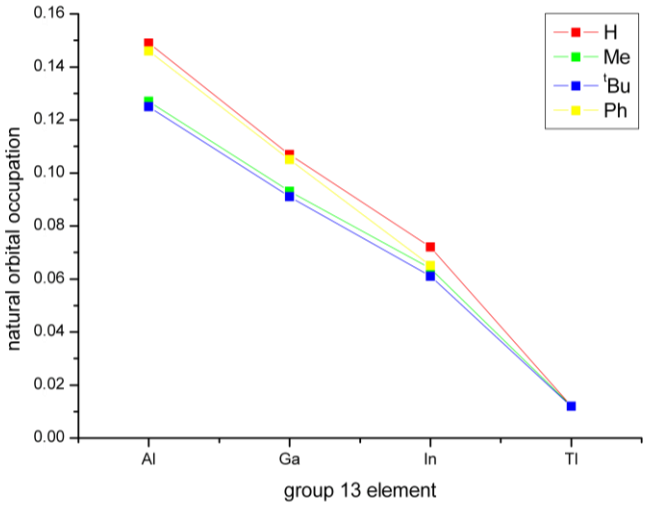

Figure 3. Calculated (CAS/cc-pVTZ) natural orbital occupations for **1**–**4**.

Before continuing with the energy and electron density analyses of **1**–**4**, it is instructive to summarize the current findings regarding bonding in group 13 dimetallenes. As the various wave function analyses illustrate, digallenes and dialuminenes in particular have a noticeable singlet diradical component in their electronic structures that plays a large role in determining the strength of the total bonding interaction. For the heavier group 13 dimetallenes, the significance of the closed shell metal−metal attraction (dispersion) increases considerably, even to the extent that it is the sole bonding contribution in dithallenes. The importance of the singlet diradical component is not all surprising from a point of view that the analogous diboronenes have a triplet ground state and have only been observed in low temperature matrices[49] although they can be isolated as carbene complexes.[50] Moreover, attempts to grow crystals of a putative terphenyl dialuminene lead to a [2+4] cycloaddition reaction with a molecule of solvent (toluene).[17] Similar reactivity is typical for singlet diradicals such as singlet oxygen, which lends strong support to the conclusion that diradical character is particularly important for both bonding and chemistry of dialuminenes. To test this hypothesis further, vertical singlet-triplet gaps were calculated for the group 13 dimetallenes with ^{t}Bu substituents. The results show that the singlet state is stabilized only by 78 kJ mol^{-1} in case of aluminum, whereas the stabilization is somewhat higher for digallenes and diindenes (97 and 103 kJ mol^{-1}, respectively) and especially for dithallenes (140 kJ mol^{-1}). Nevertheless, all of the calculated singlet-triplet gaps are rather small, which is fully on par with the calculated diradical component. However, it should be noted that in the triplet state, it is the LUMO of **1**–**4** which becomes populated by one electron and not LUMO+1 that is involved in the singlet diradical ground state. Therefore, the singlet-triplet gaps cannot be directly translated to an estimate of singlet diradical character.

Taking all of the above into consideration, the performance of the different computational methods in modeling dimetallenes can be rationalized in a straightforward manner. Clearly, either high-level ab initio methods or DFT need to be used in order to obtain consistent results. However, there is an important caveat to note. Some error compensation effects are clearly working in favor of DFT as the method performs acceptably for dithallenes even without a proper treatment of dispersion. In addition, the inclusion of dispersion effects via empirical correction term gave inconsistent results for diindenes, which casts some doubt on the accuracy of the atomic parameters used in the computational procedure.

Binding energies. Table 2 lists the calculated binding energies for dimers **1**–**4** at different levels of theory. What is evident from the data is that, at least when using the B3LYP functional, the calculated binding energies of the dimers do not change significantly when the size of the substituent is increased from methyl to phenyl. This was to be expected since none of the studied dimetallenes experiences any significant steric crowding. The calculated energies show a decreasing trend as the size of the group 13 element increases, in good agreement with the conclusions made based on wave function analyses. Compared to the B3LYP values, the binding energies at the HF level clearly illustrate how small the orbital contribution to the interaction energy is: for all but the parent dimetallenes, the dimers are at best only around 10 kJ mol^{-1} more stable than the monomers. Hence, there can be hardly any doubt about the relative importance of the slipped π-type HOMO to bonding in any of the systems **1**–**4** with realistic substituents, that is, other than hydrogen. Conversely, the interaction energies calculated using the unrestricted (broken symmetry) HF solutions compare somewhat more favorably with the B3LYP values as the method includes a zeroth-order treatment of the diradical component. In any case, the CCSD(T) approach represents theoretically the most accurate of the different methods employed, and the calculated energies are in excellent agreement with the B3LYP results. The only exception is observed for dithallenes for which the B3LYP gets a bonding interaction that is (in relative terms) considerably stronger than at the CCSD(T) level, although the predicted geometries are comparable. It is therefore likely that there is favorable error compensation at work in the B3LYP functional, which artificially strengthens the thallium–thallium interaction even in the absence of a proper dispersion correction.

In order to quantify the strength of the metal–metal interaction in **1**–**4**, the CCSD(T) and B3LYP energies in Table 2 can be compared with reference values for bond dissociation energies of E–E bonds in $H_2E–EH_2$ (Al, 219 kJ mol^{-1}; Ga, 242 kJ mol^{-1}; In, 203 kJ mol^{-1}; Tl, 164 kJ mol^{-1}),[51] which gives an energy based estimation of the bond order. Such comparison gives bond orders close to 0.3 for dialuminenes, 0.2 for digallenes, 0.15 for diindenes and roughly around 0.1 for dithallenes. These numbers reproduce well the qualitative picture given by the wave function analyses and lend strong support to the view that the bonding in group 13 dimetallenes is by all standards considerably weaker than in a typical single bond. The results are further corroborated by a recent energy based analysis of multiple bonding in main group compounds[52] as well as the in-depth investigations of digallenes with

terphenyl ligands that showed that the interaction remains weak also in experimentally characterizable systems.[14]

Table 2. Binding Energies (in kJ mol^{-1}) calculated for **1**–**4** at Different Levels of Theory

	method	H	Me	^{t}Bu	Ph
Al	HF	25	15	11	12
	UHF	40	46	25	19
	B3LYP	63	47	45	47
	CCSD(T)	64	50	-	-
Ga	HF	17	11	9	8
	UHF	35	25	11	8
	B3LYP	52	41	41	39
	CCSD(T)	51	41	-	-
In	HF	8	7	6	3
	UHF	8	11	11	3
	B3LYP	31	28	29	23
	CCSD(T)	30	24	-	-
Tl	HF	*	*	*	*
	UHF	*	*	*	*
	B3LYP	18	18	23	*
	CCSD(T)	10	10	-	-

* The optimized structure is not a minimum on the potential energy surface.

Electron density analyses. The bonding in group 13 dimetallenes has been analyzed previously using two common methods based on the total electron density: the theory of atoms in molecules (AIM) and the analysis of the electron localization function (ELF).

In the theory of AIM, the gradient field of the electron density ρ(r) is used to divide the total electron density into atomic basins.[31] Atomic populations can be obtained by direct integration of the

electron density over each basin, whereas the Fermi correlation between two basins A and B, F(A,B), as obtained from the pair density, gives the number of electrons referenced to atom A that are delocalized onto atom B. A direct measure of the number of shared electron pairs between two basins, known as the delocalization index δ, can then be obtained by summing up the contributions F(A,B) and F(B,A). Delocalization indices have been reported for the parent dialuminene and digallene,[11f,11j,53] and the calculated numbers are slightly below one which has been interpreted as a metal–metal interaction corresponding to a single bond. However, as pointed out on several occasions,[54] the delocalization index is not a measure of a covalent bond order and, therefore, should not be used as one. For conventional non-polar interactions, the delocalization indices recover the Lewis model, especially when calculated at the HF level, but the situation is not as straightforward for more complex systems as the index does not vanish completely even in cases when the atoms in question are separated by more than one bond.

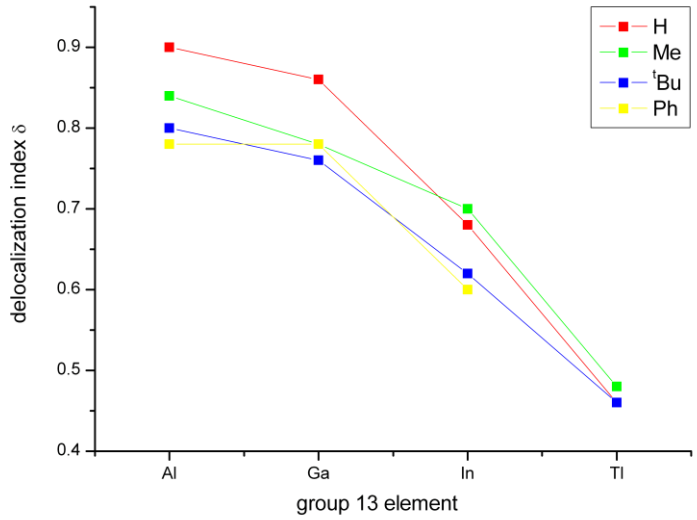

Figure 4. Calculated (B3LYP/cc-pVTZ) AIM delocalization indices for **1**–**4**.

The calculated AIM delocalization indices (at the B3LYP/cc-pVTZ level) for **1**–**4** are shown graphically in Figure 4. The results clearly mirror the already established trends and predict that less electron density is being shared between the metal atoms as the size of the group 13 element increases. The calculated values for the dithallenes, close to half a pair, seem surprisingly large, especially when

considering that the systems are unbound at the HF level which does include Fermi correlation effects (antisymmetrization). However, as noted above, the delocalization index is not a covalent bond order and therefore never zero, not even for cases where there is clearly no conventional covalent bond. As an illustrative example, the B3LYP delocalization index for the weakly (dispersion) bound dimer $I_3P\cdots PI_3$ at its optimized geometry (r_{PP} = 2.80 Å) is 0.35 electron pairs.[55] The energy of the interaction is, however, around 15 kJ mol^{-1} which is only a fraction of the strength of a typical phosphorus−phosphorus single bond. Clearly the delocalization index does not translate to a covalent bond order of the same magnitude as there is no conventional orbital contribution to bonding. In a similar fashion, the delocalization indices calculated for the group 13 dimetallenes capture features from the pair density that do not directly relate to the orbital description on which the formal bond orders are based on. Hence, if delocalization indices are to be used as an estimate of bond order in group 13 dimetallenes, the calculated numbers need to be scaled by *e.g.* subtracting the value calculated for the dithallenes from the rest of the data. This procedure yields bond orders that correlate with the importance of the diradical structure **A'** to the overall interaction, which underpins the established notion that bonding in group 13 dimetallenes is, at best, much weaker than a single bond.

Like the results given by the AIM theory, inconsistencies appear in the ELF based bonding analyses of group 13 dimetallenes. The ELF, η, is a relative measure of electron localization based on the Pauli principle, as given by the ratio of the excess kinetic energy density due to the Fermi hole and the kinetic energy density in a uniform electron gas of the same density.[32] Since ELF is a scalar function, a topological analysis of its gradient field can be used to partition the molecular space into core and valence basins. For main group element compounds, the number, population and synaptic order (the number of connections to core basins) of the valence basins generally correlate well with the qualitative domains of the VSEPR model.[56] It is therefore somewhat surprising that the ELF data for the parent dialuminene reveals a disynaptic metal−metal basin with a population of less than one electron, but the interaction is nevertheless inferred to be stronger than a single bond.[53] Even more confusing are the results for the parent digallene, which show two disynaptic gallium−gallium basins with a population of 2.25 electrons each, indicative of a bond order even above two.[11j]

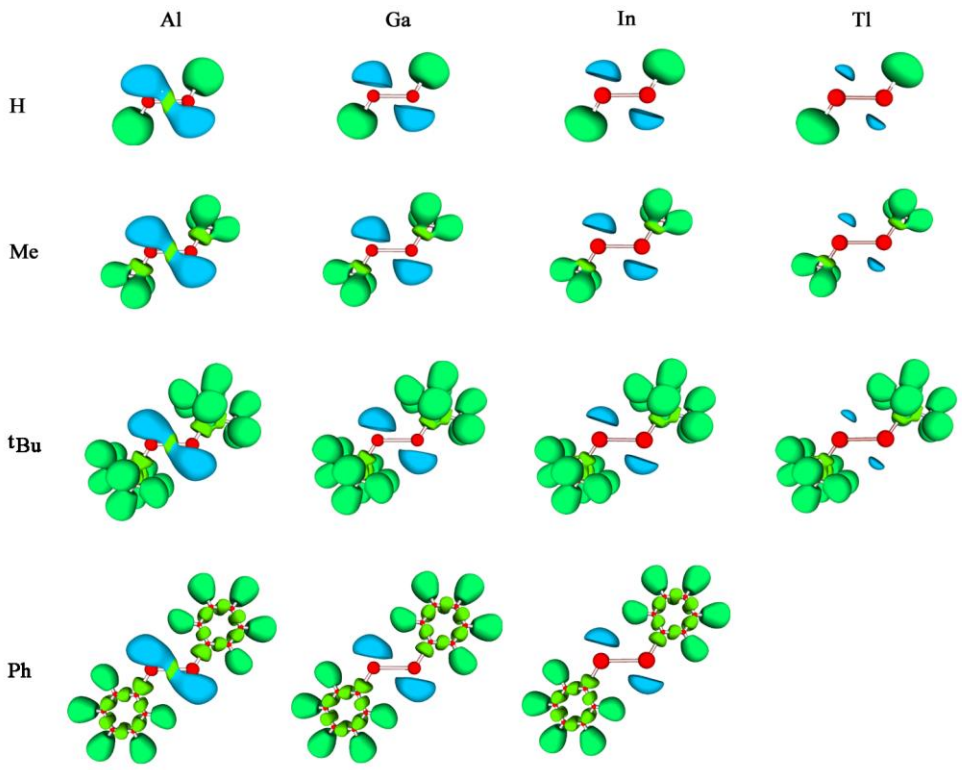

Figure 5. Calculated (B3LYP/cc-pVTZ) ELF plots of **1**–**4** (η = 0.7); basin color code: core = red, lone pair = blue, bonding = green.

The results from the ELF analyses (at the B3LYP/cc-pVTZ level) of **1**–**4** are given in Table 3 (basin populations) and Figure 5 (ELF isosurfaces). As expected, a distinct disynaptic metal–metal basin whose attractor is centered between the two group 13 nuclei could only be found for dialuminenes. In case of digallenes, the topological partitioning of the ELF yields two V(Ga,Ga) basins, as reported before,[11j] but a closer look to their attractors reveals an atypical pattern for a doubly bonded species: the attractors are not located on the mid-bond plane, symmetrically above and below the nuclear axis but instead precisely at the positions expected for two lone pairs, one on each gallium atom. Clearly, the V(Ga,Ga) basins need to be interpreted as two lone pair basins that are just on the hinge of separation. This view is corroborated by the ELFs calculated for diindenes and dithallenes that show no indication of a significant bonding interaction between the group 13 elements and exhibit two purely monosynaptic lone pair basins. Moreover, for all dialuminenes except the parent system, the two

monosynaptic V(Al) basins appear as disynaptic V(Al,Al) bonding basins in the analysis. Hence, rather than representing a bizarre anomaly, the ELF of digallenes fits perfectly to the observed trends when all pieces of the puzzle are evaluated simultaneously. It needs to be remembered that the attribution of ELF basins to conceptual chemical descriptors is, at least for the time being, purely empirical one and has to be thoroughly investigated in each case.

The properties of the ELF basins calculated for **1**–**4** also correlate well with the bonding description established above. For dialuminenes, the picture portrayed by the calculated basin populations shows that the aluminum-aluminum bond order is roughly one half, whereas the lone pair population is approximately 1.50 electrons. The amount of electrons in the bonding basin is the greatest for the parent dialuminene, which has the largest orbital component to bonding, and slightly smaller but nearly equal for all the other derivatives. For digallenes, the weight of the diradical structure **A'** in the wave function is smaller than in the case of dialuminenes, but it still affects the bonding as exemplified by the disynaptic nature of the two lone pair basins. For diindenes and dithallenes, the Lewis structure **A** totally dominates the wave function, which is mirrored in their ELFs, having no contribution from disynaptic metal–metal bond basins. Interestingly, the number of electrons in the lone pairs of digallenes and diindenes is somewhat greater than two as some core contribution becomes mixed in. This result is, however, fully in line with the analysis of the monomeric gallium(I) and indium(I) species, which display a comparable distribution of electrons among their ELF basins.

Table 3. Summary of Results from Electron Localization Function Analysis of **1**–**4**[a]

	basin	H	Me	^{t}Bu	Ph
Al	V(Al,Al)	0.83 (0.71)	0.70 (0.76)	0.67 (0.78)	0.69 (0.76)
	V(Al)	1.53 (0.47)	1.66 (0.45)	1.69 (0.46)	1.66 (0.46)
Ga	V(Ga)	2.17 (0.55)	2.23 (0.54)	2.28 (0.55)	2.25 (0.55)
In	V(In)	2.06 (0.60)	2.15 (0.59)	2.18 (0.60)	2.13 (0.60)
Tl	V(Tl)	1.64 (0.67)	1.67 (0.66)	1.56 (0.68)	-

[a] Average basin populations and their relative fluctuations (in parenthesis).

4 Conclusions

The electronic structures of group 13 dimetallenes **1–4** were analyzed using different quantum chemical methods. The current study represents the first systematic attempt to determine the changes in bonding in these systems by a function of two variables: the identity of the metal and the organic substituent. The most important conclusions drawn from the results are as follows:

(1) The electronic structures of group 13 dimetallenes represent a delicate interplay between static and dynamic electron correlation effects. In dialuminenes, the bonding is dictated primarily by diradical character, which, however, is only moderate. In the heaviest thallium congeners, the closed shell attraction (dispersion) solely dominates the total interaction. Both digallenes and diindenes fall in between these two extremes. The orbital (donor-acceptor) interaction plays only a small role in the overall metal−metal bonding. The only exception to this generalization are the parent systems (R = H) which do gain important stabilization through secondary orbital interactions between the lone pairs on the group 13 element and the E−H bonds facing them.

(2) In order to obtain meaningful results from theoretical calculations, the chosen level of theory needs to be able to give a balanced description of all important bonding contributions. In this respect, high-end ab initio methods, such as coupled cluster and complete active space, are the most viable. DFT offers a computationally cost-effective alternative which is, however, not as theoretically trustworthy for diindenes and dithallenes due to difficulties in treatment of dispersion effects. Although second order perturbation theory works for dithallenes, it should not be used to describe the electronic structures of the lighter members of the series because of their singlet diradical nature.

(3) When all the important bonding interactions in group 13 dimetallenes are accounted for and the acquired theoretical data evaluated in detail, the results from different bonding analyses are in perfect harmony and indicate that the metal−metal bond in group 13 dimetallenes is very weak. For dithallenes, the formal bond order is close to zero, whereas for dialuminenes it is roughly about one half. These results are on par with the determined X-ray crystal structures and cryoscopic measurements which show significantly elongated metal−metal distances and dissociation of the heavier dimetallenes into monomers in solution, respectively.

(4) The view of bonding in group 13 dimetallenes established by the current investigations lends significant support for the interpretation of the related (free) dialuminyne and digallyne as dianions with a formal bond order significantly lower than three. As the two additional electrons occupy a purely π-bonding LUMO of the neutral dimetallenes, the metal−metal bond order in the free dianions can be expected to be roughly around 1.5. This because the diradical nature of dimetallenes involves the higher energy LUMO+1 orbital and therefore plays an important role in the corresponding dialuminynes and digallynes as well. The multiconfigurational nature of digallynes[11h] and the presence of only two shared electron pairs in the Ga–Ga bond[11f] have already been noted in the literature, but the results of these investigations have been largely disregarded thus far in lieu of competing interpretations favoring a triple bond formulation

Based on the results of this study, we also anticipate that singlet diradical character, or near degeneracy effects, may play a more prominent role in explaining weak interactions in inorganic molecules than hitherto recognized.

Acknowledgement. We are grateful to the National Science Foundation (CHE-0948417), the University of Jyväskylä, and the Academy of Finland for financial support of this research.

Supporting Information Available. Optimized geometries (in standard xyz format) of **1**–**4**.

References and Notes

[1] (a) Davidson, P. J.; Lappert, M. F. *Chem. Commun*. **1973**, 317; (b) Goldberg, D. E.; Harris, D. H.; Lappert, M. F.; Thomas, K. M. *Chem Commun*. **1976**, 261.

[2] West, R.; Fink, M. J.; Michl, J. *Science* **1981**, *214*, 1343.

[3] Yoshfuji, M.; Shima, I.; Inamoto, N.; Hirotsu, K.; Higuchi, T. *J. Am. Chem. Soc.* **1981**, *103*, 4587.

[4] Kutzelnigg, W. *Angew. Chem., Int. Ed. Engl.* **1984**, *23*, 272.

[5] (a) Power, P. P. *Chem. Rev.* **1999**, *99*, 3463. (b) Power, P. P. *Chem. Commun.* **2003**, 2091. (c) Weidenbruch, M. *Angew. Chem., Int. Ed.* **2003**, *42*, 2222. (d) Weidenbruch, M. *Angew. Chem., Int. Ed.*

2005, *44*, 514. (e) Rivard, E.; Power, P. P. *Inorg. Chem.* **2007**, *46*, 10047. (f) Sasamori, T.; Tokitoh, N. *Dalton Trans.* **2008**, 1395. (g) Wang, Y.; Robinson G. H. *Chem. Commun*. **2009**, 5201.

[6] (a) Klusik H.; Berndt, A. *Angew. Chem., Int. Ed. Engl*. **1981**, *20*, 870. (b) Berndt, A.; Klusik, H.; Fichtner, W. *J. Organomet. Chem.* **1981**, *222*, C25.

[7] (a) Pluta, C.; Pörschke, K.-R.; Krüger, C.; Hildenbrand, K. *Angew. Chem., Int. Ed. Engl*. **1993**, *32*, 388. (b) Uhl, W.; Vester, A.; Kaim, W.; Poppe, J. *J. Organomet. Chem*. **1993**, *454*, 9. (c) He, X.; Barlett, R.. A.; Olmstead, M. M.; Ruhlandt-Senge, K.; Sturgeon, B. E.; Power, P. P. *Angew. Chem., Int. Ed. Engl*. **1993**, *32*, 717.

[8] (a) Power, P. P. *Inorg. Chim. Acta*. **1992**, *198-200*, 443. (b) Wehmschulte, R. J.; Power, P. P. *Angew. Chem., Int. Ed*. **1998**, *37*, 3152.

[9] (a) Wiberg, N.; Amelunxen, K.; Nöth, H.; Schwenk, H.; Kaim. W.; Klein, A.; Scheiring, T. *Angew. Chem., Int. Ed. Engl.* **1997**, 36, 1213. (b) Wiberg, N.; Blank, T.; Amelunxen, K.; Noth, H.; Knizeck, J.; Habereder, T.; Kaim, W.; Wanner, M. *Eur. J. Inorg. Chem*. **2001**, 1719.

[10] Su, J.; Li, X.-W.; Crittendon, R.. C.; Robinson, G. H. *J. Am. Chem. Soc.* **1997**, *119*, 5471.

[11] (a) Kinkhammer, K. W. *Angew. Chem., Int. Ed. Engl.* **1997**, *36*, 2320. (b) Xie, Y.; Grev, R. S.; Gu, J.; Schaefer, H. F., III; Schleyer, P. v. R.; Su, J.; Li, X.-W.; Robinson, G. H. *J. Am. Chem. Soc.* **1998**, *120*, 3773. (c) Cotton, F. A.; Cowley, A. H.; Feng, X. *J. Am. Chem. Soc*. **1998**, *120*, 1795. (d) Allen, T. L.; Fink, W. H.; Power, P. P. *J. Chem. Soc., Dalton Trans*. **2000**, 407. (e) Grützmacher, H.; Fässler, T. F. *Chem. Eur. J*. **2000**, *6*, 2317. (f) Molina, J. M.; Dobado, J. A.; Heard, G. I.; Bader, R. F. W.; Sundberg, M. R. *Theor. Chem. Acc*. **2001**, *105*, 365. (g) Bridgeman, A. J.; Ireland, L. R. *Polyhedron* **2001**, *20*, 2851. (h) Takagi, N.; Schmidt, M. W.; Nagase, S. *Organometallics* **2001**, *20*, 1646. (i) Himmel, H.-J.; Schnöckel, H. *Chem. Eur. J*. **2002**, *8*, 2397. (j) Chesnut, B. D. *Heteroat. Chem*. **2003**, *14*, 175. (k) Ponec, R.; Yuzhakov, G.; Gironés, X.; Frenking, G. *Organometallics* **2004**, *23*, 1790.

[12] Hardman, N. J.; Wright, R. J.; Phillips, A. D.; Power P. P. *Angew. Chem., Int. Ed.* **2002**, *41*, 2842.

[13] (a) Uhl, W.; Hiller, W.; Layh, M.; Schwarz, W. *Angew. Chem., Int. Ed. Engl.* **1992**, *31*, 1364. (b) Uhl, W.; Jantschak, A. *J. Organomet. Chem.* **1998**, *555*, 263.

[14] Zhu, Z.; Fischer, R. C.; Ellis, B. D.; Rivard, E.; Merrill, W. A.; Olmstead, M. M.; Power, P. P.; Guo, J. D.; Nagase, S.; Pu, L. *Chem. Eur. J*. **2009**, *15*, 5263.

[15] Wright, R. J.; Phillips, A. D.; Hardman, A. D.; Power, P. P. *J. Am. Chem. Soc*. **2002**, *124*, 8538.

[16] Wright, R. J.; Phillips, A. D.; Hino, S.; Power, P. P. *J. Am. Chem. Soc*. **2005**, *127*, 4794.

[17] Wright, R. J.; Phillips, A. D.; Power, P. P. *J. Am. Chem. Soc*. **2003**, *125*, 10784.

[18] (a) Treboux, G.; Barthelat, J. C. *J. Am. Chem. Soc*. **1993**, *115*, 4870. (b) Trinquier, G.; Malrieu, J.-P. *J. Am. Chem. Soc.* **1987**, *109*, 5303. (c) Malrieu, J.-P.; Trinquier, G. *J. Am. Chem. Soc.* **1989**, *111*, 5916. (d) Carter, E. A.; Goddard, W. A. III *J. Phys. Chem.* **1986**, *90*, 998.

[19] Pyykkö, P. *Chem. Rev.* **1997**, *97*, 597.

[20] (a) Raghavachari, K.; Anderson, J. B. *J. Phys. Chem.* **1996**, *100*, 12960. (b) Tew, D. P; Klopper W.; Helgaker T. *J. Comput. Chem.* **2007**, 28, 1307.

[21] Møller, C.; Plesset, M. S. *Phys. Rev*. **1934**, *46*, 618.

[22] (a) Raghavachari, K.; Trucks, G. W.; Pople, J. A.; Head-Gordon, M. *Chem. Phys. Lett.* **1989**, *157*, 479. (b) Hampel, C.; Peterson, K.; Werner, H.-J. *Chem. Phys. Lett*. **1992**, *190*, 1. (c) Deegan, M. J. O; Knowles, P. J. *Chem. Phys. Lett.* **1994**, *227*, 321.

[23] (a) Roos, B. E.; Taylor, P. R.; Siegbahn, P. E. M. *Chem. Phys.* **1980**, *48*, 157. (b) Werner, H. J.; Knowles. P. J. *J. Chem. Phys*., **1985**, *82*, 5053. (c) Knowles, P. J.; Werner, H.-J. *Chem. Phys. Lett*., **1985**, *115*, 259.

[24] (a) Andersson, K.; Malmqvist, P.-Å.; Roos, B. O. *J. Chem. Phys.* **1992**, *96*, 1218. (b) Celani, P.; Werner, H.-J. *J. Chem. Phys*., **2000**, *112*, 5546.

[25] (a) Becke, A. D. *J. Chem. Phys*. **1993**, *98*, 5648. (b) Lee, C.; Yang, W.; Parr, R. G. *Phys. Rev. B* **1998**, *37*, 785. (c) Vosko, S. H.; Wilk, L.; Nusair, M. *Can. J. Phys.* **1980**, *58*, 1200. (d) Stephens, P. J.; Devlin, F. J.; Chabalowski, C. F.; Frisch, M. J. *J. Phys. Chem.* **1994**, *98*, 11623.

[26] Zhao, Y.; Truhlar, D. G. *Theor. Chem. Acc*. **2008**, *120*, 215.

[27] Grimme, S. *J. Comput. Chem.* **2004**, *12*, 1463.

[28] (a) Dunning, T. H. Jr. *J. Chem. Phys*. **1989**, *90*, 1007. (b) Woon, D. E.; Dunning, T. H. Jr. *J. Chem. Phys*. **1993**, *98*, 1358. (c) Wilson, A. K.; Woon, D. E.; Peterson, K. A.; Dunning, T. H. Jr. *J. Chem. Phys*. **1999**, *110*, 7667.

[29] (a) Peterson, K. A. *J. Chem. Phys*. **2003**, *119*, 11099. (b) Metz, B.; Schweizer, M.; Stoll, H.; Dolg, M.; Liu, W. *Theor. Chem. Acc.* **2000**, *104*, 22. (c) Metz, B.; Stoll, H.; Dolg, M. *J. Chem. Phys.* **2000**, *113*, 2563.

[30] Boys, S. F.; Bernardi, F. *Mol. Phys*. **1970**, *19*, 553.

[31] (a) Biegler-Konig, F. W.; Nguyen-Dang, T. T.; Tal, Y.; Bader, R. F. W.; Duke, A. J. *J. Phys. B* **1981**, *14*, 2739. (b) Bader, R. F. W.; Nguyen-Dang, T. T. *Adv. Quantum Chem*. **1981**, *14*, 63.

[32] (a) Silvi, B.; Savin, A. *Nature* **1994**, *371*, 683 (b) Savin, A.; Becke, A. D.; Flad, J.; Nesper, R.; Preuss, H.; Schnering, H. G. *Angew. Chem., Int. Ed. Engl*. **1991**, *30*, 409 (c) Savin, A.; Nesper, R.; Wengert, S.; Fässler, T. F. *Angew. Chem., Int. Ed. Engl*. **1997**, *36*, 1808.

[33] Frisch, M. J. et al. *Gaussian 09*, Revision A.2; Gaussian, Inc.: Wallingford, CT, USA, 2009.

[34] *MOLPRO* (version 2006.1), a package of ab initio programs,Werner, H.-J.; Knowles, P. J.; Lindh, R.; Manby, F. R.; Schütz, M. and others, see http://www.molpro.net.

[35] Noury, S.; Krokidis, X.; Fuster, F.; Silvi, B. TopMoD, Université Pierre et Marie Curie, Paris, France, 1997.

[36] (a) Laaksonen, L. *J. Mol. Graph*. **1992**, *10*, 33. (b) Bergman D. L.; Laaksonen, L.; Laaksonen A. *J. Mol. Graph*. **1997**, *15*, 301.

[37] (a) Adams, W. H. *Phys. Rev.* **1962**, *127*, 1650. (b) Mayer, I.; Löwdin, P. O. *Chem. Phys. Lett.* **1993**, *202*, 1. (c) Čížek, P.; Paldus, J. *J. Chem. Phys.* **1967**, *47*, 3976.

[38] Bally, T.; Borden, W. T. In *Calculation on Open-Shell Molecules: A Beginner's Guide*, Lipkowitz, K. B., Boyd, D. B., Eds.; Reviews in Computational Chemistry, 13; Wiley-VCH: New York, 1999; p 1.

[39] In principle, valence bond theory could also be used as it takes into account static electron correlation effects. See for example, Gerratt, J.; Cooper, D. L.; Karadakov, P. B.; Raimondi, M. *Chem. Soc. Rev.* **1997**, *26*, 87.

[40] (a) Jung, Y.; Brynda, M.; Power, P. P.; Head-Gordon, M. *J. Am. Chem. Soc.* **2006**, *128*, 7815. (b) Power, P. P. *Organometallics* **2007**, *26*, 4362.

[41] Cremer, D. *Mol. Phys.*, **2001**, *99*, 1899.

[42] Hayes, E. F.; Siu, A. K. Q. *J. Am. Chem. Soc*. **1971**, *93*, 2090.

[43] Musial, M.; Bartlett, R. J. *Rev. Mod. Phys.* **2007**, *79*, 291.

[44] Löwdin, P.-O. *Phys. Rev.* **1955**, *97*, 1474.

[45] Gordon, M. S.; Schmidt, M. W.; Chaban, G. M.; Glaesemann, K. R.; Steevens, W. J.; Gonzalez, C. *J. Chem. Phys.* **1999**, *110*, 4199.

[46] Pople, J. A.; Head-Gordon, M.; Raghavachari, K. *J. Chem. Phys.* **1987**, *87*, 5968.

[47] (a) Flynn, C.; Michl, J. *J. Am. Chem. Soc.* **1974**, *96*, 3280. (b) Dohnert, D.; Koutecky, J. *J. Am. Chem. Soc.* **1980**, *102*, 1789. (c) Bonacic-Koutecky, V.; Koutecky, J.; Michl, J. *Angew. Chem., Int. Ed. Engl.* **1987**, *26*, 170.

[48] (a) Pulay, P.; Hamilton, T. P. *J. Chem. Phys*. **1988**, *88*, 4926. (b) Bofill, J. M.; Pulay, P. J. *Chem. Phys*. **1989**, *89*, 3637. (c) Wolinski, K.; Pulay, P. *Chem. Phys*. **1989**, *90*, 3647.

[49] (a) Knight, L. B., Jr.; Kerr, K.; Miller, P. K.; Arrington, C. A. *J. Phys. Chem.* **1995**, *99*, 16842.

[50] (a) Wang, Y.; Quillian, P.; Wei, P.; Wannene, C. S.; Xie, Y.; King, R. B.; Schaefer, H. F.; Schleyer, P. v. R; Robinson, G. H. *J. Am. Chem. Soc.* **2007**, *129*, 12412. (b) Wang. Y.; Quillian, B.; Wei, P.; Xie Y.; Wannere, C. S.; King, R. B.; Schaefer, H. F. III; Schleyer, P. v. R.; Robinson, G. H. *J. Am. Chem. Soc*. **2008**, *130*, 3298.

[51] Szabó, A.; Kovács, A.; Frenking, G. *Z. Anorg. Allg. Chem.* **2005**, *631*, 1803.

[52] Schnöckel, H.; Himmel, H.-J. *Chem. Eur. J*. **2003**, *9*, 748.

[53] Chesnut, D. B. *Chem. Phys.* **2006**, *321*, 269.

[54] (a) Bader, R. F. W.; Stephens, M. E. *J. Am. Chem. Soc.* **1975**, *97*, 7391. (b) Fradera, X.; Austen, M. A.; Bader, R. F. W. *J. Phys. Chem. A* **1999**, *103*, 304. (c) Poater, J.; Duran, M.; Solà, M.; Silvi, B. *Chem. Rev.* **2005**, *105*, 3911.

[55] Moilanen, J.; Ganesamoorthy, C.; Balakrishna, M. S.; Tuononen, H. *Inorg. Chem*. **2009**, *48*, 6740.

[56] Gillespie, R. J. *Coord. Chem. Rev.* **2008**, *252*, 1315.